# Supporting Information:

# Ballistic transport and electrical spin signal amplification in a three-terminal spintronic device

Lei Zhu and Edward T. Yu

Department of Electrical and Computer Engineering

Microelectronics Research Center

The University of Texas at Austin

Austin, TX 78758

**Section A: Magnetic force microscopy measurements on Co contacts**

To confirm that each Co contact has single-domain magnetization along the long axis of the contact, and that the coercive fields for magnetization reversal are different for contacts of different widths, due to shape anisotropy effects, we have used magnetic force microscopy to measure the magnetization as a function of external applied magnetic field, as shown in Figure S1. Single-domain magnetization of each Co contact is evident in Figure S1(c)-(f), with a transition in magnetization from an all-parallel configuration at external fields up to 400 Oe (Figure S1(c)-(d)), to an antiparallel configuration at 600-800 Oe external field (Figure S1(e)), and back to a parallel configuration, but with magnetization in the opposite direction, at 800 Oe and above (Figure S1(f)).

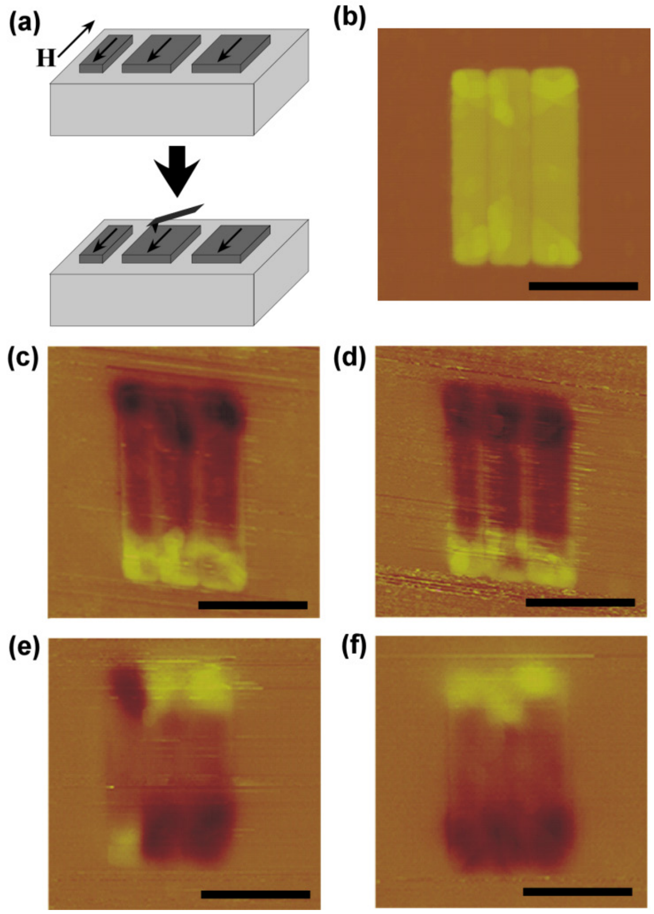


**Figure S1.** (a) Schematic diagram of room-temperature magnetic force microscopy (MFM) measurement process: an external magnetic field is applied to control the magnetization of the Co contacts, and subsequently MFM measurements are performed to assess directly the contact magnetization as a function of external field. (b) Atomic force microscope topographic and (c)-(f) MFM images of the Co contacts following application of successively larger external fields (-2000 Oe, +300 Oe, +600 Oe, and +1200 Oe, respectively), showing the transition from an all-parallel magnetization configuration (c)-(d) to an antiparallel configuration (e) and back to an all-parallel configuration (f). All scale bars are 1μm.

**SectionB: Spin-dependent analysis of ballistic transport**

As noted in the main text, the total charge current $I_L$ including both spin up and spin down channels is given by

$$I_L = \sum_{\alpha,\beta} (I_{LC}^{\alpha\beta} + I_{LR}^{\alpha\beta}) = \frac{e}{h} \sum_{\alpha,\beta} \int dE \{ T_{LC}^{\alpha\beta} [f_L(E) - f_C(E)] + T_{LR}^{\alpha\beta} [f_L(E) - f_R(E)\} , \qquad \text{(S.1)}$$

where $T_{LC}^{\alpha\beta}$ and $T_{LR}^{\alpha\beta}$ represent the transmission probabilities from spin channel $\alpha$ in the left terminal to spin channel $\beta$ in the center terminal and the right terminal, respectively. $f_L(E)$, $f_C(E)$ and $f_R(E)$ refer to the Fermi distribution functions in the left, center, and right terminals. We represent the transmission probabilities in Eq. (S.1) by linear conductances $G_{LC}^{\alpha\beta} = \frac{e^2}{h} T_{LC}^{\alpha\beta}$ and $G_{LR}^{\alpha\beta} = \frac{e^2}{h} T_{LR}^{\alpha\beta}$ , with these conductances including all effects of device geometry on transmission and reflection between spin-selective terminals. This linear approximation is appropriate for our analysis, since within the small range of applied voltages of interest in operation of this device, the conductance can be treated as constant due to its very gradual variation with voltage. Assuming the low temperature limit for the Fermi distribution $f(E)$, we can simplify Eq. (S.1) to the form

$$I_L = \sum_{\alpha,\beta} (G_{LC}^{\alpha\beta} (V_L - V_C) + G_{LR}^{\alpha\beta} (V_L - V_R)) . \qquad \text{(S.2)}$$

Employing a standard procedure[1] to compute the conductances $G_{LC}^{P(AP)}$ and $G_{LR}^{P(AP)}$ , we obtain

$$\frac{\Delta G_{LC}}{\overline{G}_{LC}} \equiv \frac{\left(G_{LC}^{P} - G_{LC}^{AP}\right)}{\left(G_{LC}^{P} + G_{LC}^{AP}\right)/2} \approx \left(\frac{\gamma^2}{1-\gamma^2}\right)\left(\frac{1}{1+\tau_n/\tau_{sf}}\right) \approx \frac{\gamma^2}{1-\gamma^2} , \qquad \text{(S.3)}$$

where $\gamma$ is the interface spin-asymmetry coefficient and can be determined for our devices from two-terminal spin valve measurements.[1] For the channel lengths and bias voltages employed in our devices, the typical electron mobility of 6000 $cm^2/(V\cdot s)$ we have measured for electrons in the InAs surface electron layer implies that the mean electron transit time across the channel, $\tau_n$, is in the range of 0.06 ps, which is much smaller than the reported electron spin lifetime $\tau_{sf}$ for surface electrons in InAs of 0.8 ps.[2] This justifies the assumption of ballistic transport between adjacent contacts in our analysis.

For transport between the left and right terminals, the electron spin polarization will decay exponentially with path length $l$ between the terminals, and will therefore be proportional to $\exp(-l/L_{sf})$, where $L_{sf}$ is the spin diffusion length. For the device studied here, the path length between the right and left contacts, $L_{LR}$, may be taken to be the center-to-center contact separation, ~550nm. This exponential dependence then yields

$$\frac{\Delta G_{LR}}{\overline{G}_{LR}} = \frac{\Delta G_{LC}}{\overline{G}_{LC}} \exp\left(-\frac{L_{LR}}{L_{sf}}\right) \tag{S.4}$$

The change in $I_L$ that occurs upon changing the magnetization of the left contact relative to that of the center and right contacts is given by

$$\Delta I_L = (G_{LC}^P - G_{LC}^{AP})(V_L - V_C) + (G_{LR}^P - G_{LR}^{AP})(V_L - V_R) = \Delta G_{LC}(V_L - V_C) + \Delta G_{LR}(V_L - V_R). \tag{S.5}$$

Assuming operation at a bias point for which $I_L^{AP} = 0$, we finally obtain Eq. (2) from the main text,

$$\begin{aligned} \Delta I_L &\approx \Delta G_{LC}(V_L - V_C)\left[1 - \exp\left(-L_{LR}/L_{sf}\right)\right] \\ &\approx \left(\frac{\gamma^2}{1-\gamma^2}\right)\left(\frac{G_{LC}^P + G_{LC}^{AP}}{2}\right)\left(V_L - V_C\right)\left[1 - \exp\left(-L_{LR}/L_{sf}\right)\right] \end{aligned} \tag{S.6}$$

**Section C: Drift-diffusion analysis of magnetoresistance in InAs-based spin valves and three-terminal transistor devices**

Following a procedure similar to that employed for spin valve devices,[3] the spin diffusion model and spin injection coefficient $\gamma$ as deduced above can then be applied to estimate the spin-dependent signal in our multi-terminal spin transistor structure. To simplify the calculation, we exclude the effects of device geometry by assuming that the ferromagnetic terminals and InAs channels form ideal dot contacts, and channel lengths are estimated as center-to-center distances between adjacent terminals. Since such calculations without considering the geometry of spin valves will actually overestimate magnetoresistance,[4] this assumption still allows us to estimate the maximum spin-dependent signal predicted by a spin diffusion model. We also assume that the left terminal is a floating gate since the charge current through the left terminal is zero in all circumstances and the spin currents from both up/down channels compensate each other for the antiparallel magnetization configuration. Therefore, the change in current at the left terminal that occurs upon changing the contact magnetization from the parallel to antiparallel configuration is the nonzero total current from both spin up/down channels at the left terminal for the parallel magnetization configuration.

The electrochemical potentials of the spin up/down channels, $\mu_{\pm}(x)$, are given by[3]

$$\mu_{\pm}(x) = \mu_0 + \frac{j_0 e}{\sigma_n} \cdot x \pm (p \cdot \exp(-x / L_{sf}) + q \cdot \exp(x / L_{sf})) \qquad \text{(S. 7)}$$

where $\mu_0$ is the charge chemical potential, $j_0$ is the charge current density, $\sigma_n$ is the conductivity of the nonmagnetic channel, and $p$ and $q$ are constant coefficients determined by boundary conditions. Incorporating the appropriate boundary conditions at the center and right terminals, the splitting of the electrochemical potential at the center terminal is

$$\delta\mu(C) = \mu_+(C) - \mu_-(C) = 2 j_0 e \gamma \rho_N^* L_{sf} \tanh(\frac{L_{RC}}{2L_{sf}}), \tag{S. 8}$$

where $\gamma$, $\rho_N^*$, and $L_{sf}$ are the spin injection coefficient at the contact interface, the resistivity of the semiconductor channel, and the spin diffusion length inside the semiconductor channel, respectively.

The spin splitting of the electrochemical potential will decay exponentially from the center terminal to the left terminal without charge currents flowing through them. When the magnetization is switched from antiparallel to parallel, the change in current at the spin-selective left contact is then given by,

$$\Delta I_{\mathrm{L}} = \left| I_L^P - I_L^{AP} \right| = \delta\mu(L) \frac{A\gamma}{\mathrm{e}(1-\gamma^2)\mathrm{r_C}} \tag{S.9}$$

where $A$ is the contact area at the left terminal and the spin-selective contact resistance is given by $\mathrm{r}_\pm = 2(1 \mp \gamma) r_C$.

Thus, the change in current detected at left terminal, $\Delta I_L$, in this model based on diffusive spin transport is

$$\Delta I_{\mathrm{L}} = \frac{2 j_0 A \rho_N^* l_{sf}}{r_C} \tanh(\frac{L_{RC}}{2L_{sf}}) \cdot \exp\left( -\frac{L_{\mathrm{LC}}}{L_{sf}} \right) \cdot \left( \frac{\gamma^2}{1-\gamma^2} \right) \tag{S.10}$$

Substituting the values of $\gamma$ and $L_{sf}$ from our experiments,[5] the maximum estimate of $\Delta I_{\mathrm{L}}$ with the spin diffusion model is still one order of magnitude smaller than our observed results, implying that of the spin diffusion model is not an appropriate description of transport in our devices.

**Section D: Exclusion of parasitic effects in a three-terminal spin transistor**

Possible spurious sources for the electrical device behavior we observe, notably the local Hall effect (LHE)[6] and spin precession, can be eliminated by analysis of their expected effect on our devices. To exclude the possibility of the local Hall effect giving rise to the observed magnetoresistance in our devices, a set of hybrid Hall devices with Co contacts on top of InAs surface electron layers were fabricated. MFM measurements show the stray field of a rectangular magnetic contact is normally intensified at the ends of the long axis, as shown in Figure S1. For this reason, in these experiments we located the edge of the magnetic contacts in the middle of the electron transport channels to increase the local Hall effect signal arising from the perpendicular components of the stray fields from the magnetic contacts. In our measurements, no magnetization-dependent signals were detected in this set of devices. We therefore conclude that in our multi-terminal spin transistors, the perpendicular components of the stray fields from the magnetic contacts will not contribute significantly to the electron transport behaviors observed in our magnetoresistance measurements.

Spin precession is the other potential source for parasitic signals in our measurements. For the InAs surface electron layers, the dominant spin-orbit interaction mechanism is 'structure inversion asymmetry' (SIA), giving rise to the Rashba term in the Hamiltonian, $H_R = -\frac{i}{2}[\alpha\sigma \times \nabla] \cdot \hat{v}$ .[7] As the spin polarization of surface electrons is defined along the magnetization direction of the magnetic contacts, and thus perpendicular to the electron transport direction, both spin up and spin down states are treated as eigenstates of the modified Hamiltonian equation with the Rashba term included.[8] The phase difference from spin procession is then suppressed to zero. During our measurements, the external magnetic fields are nominally applied parallel to the spin polarization direction, obviating electron spin precession along the polarized axis. Since the magnetic fields may not be perfectly aligned with the spin polarization direction, their off-plane components may cause in-plane spin precession at the Larmor frequency $\Omega = g\mu_B B/\hbar$ ,where $g$ is the electron g-factor of InAs, $\mu_B$ is the Bohr magneton and $\hbar$ is the reduced Planck's constant. In the range of our applied magnetic fields, even for an extraordinarily misaligned case, for instance, a 20° misalignment between the magnetic fields and the spin polarization, the off-plane components of the magnetic fields are only able to introduce a precession of less than 10°. Therefore, the total spin precession from both the internal crystal structure of InAs and the external magnetic fields is unlikely to be observed in our measurements. When the external magnetic fields are applied fully perpendicular to the InAs surface, the spin precession is still not observable in our spin transistor devices, due to the short channel lengths and fast spin decoherence inside these devices. In our spin transistor devices, an out-of-plane magnetic field beyond 1 T would be required to induce spin precession through 180° over a channel length of ~100 nm. Such a strong magnetic field would saturate the magnetization of the Co contacts in the out-of-plane direction,[9] eliminating the in-plane spin polarization within the InAs channels upon with device operation is based. One should also note that the rapid spin decoherence will suppress spin precession.[10] Therefore, magnetoresistance oscillation is very unlikely to be observed in our devices even with strong magnetic fields.

**Reference**

[1] A. Fert, J. M. George, H. Jaffrès, and R. Mattana, *IEEE Trans. Electron Devices* **54**, 921 (2007).

[2] Ch. Schierholz, R. Kürsten, G. Meier, T. Matsuyama, and U. Merkt, *phys. stat. sol. (b)* **233**, 436 (2002).

[3] F. J. Jedema, M. S. Nijboer, A. T. Filip, and B. J. van Wees, *Phys. Rev. B* **67**, 085319 (2003).

[4] H. Dery, Ł. Cywiński; and L. J. Sham, *Phys. Rev. B* **73**, 161307 (2006).

5 L. Zhu and E. T. Yu, *J. Vac. Sci. Technol. B* **28**, 1164 (2010). .

[6] F. G. Monzon, M. Johnson, M. L. Roukes, *Appl. Phys. Lett.* **71**, 3087 (1997).

[7] S. Lamari, *Phys. Rev. B* **64**, 245340 (2001).

[8] T. Matsuyama, R. Kürsten, C. Meißner, and U. Merkt, *Phys. Rev. B* **61**, 15588 (2000).

[9] J. M. Alameda, M. C. Contreras, F. Carmona, and F. Lopez, *phys. Stat. sol. (a)* **107**, 329 (1988).

[10] X. Lou, C. Adelmann, M. Furis, S. A. Crooker, C. J. Palmstrøm, and P. A. Crowell, *Nat. Phys.* **3**, 197 (2007).